

Effect of beta and collisionality on the vacuum magnetic field islands in stellarators

L. García¹, B. A. Carreras², V. E. Lynch², M. Wakatani³

1) Universidad Carlos III, 28911 Leganés, Madrid, SPAIN

2) Oak Ridge National Laboratory, Oak Ridge, Tennessee 37831-8070, U.S.A.

3) Graduate School of Energy Science, Kyoto University, Gokasho, Uji, Japan 611-0011

e-mail contact of main author: lgarcia@fis.uc3m.es

Abstract. We have used the resistive pressure gradient driven instability model to study the effect of plasma on a vacuum magnetic field island. We have studied under what conditions the island is amplified or reduced. Starting with a set of reference parameters, we have varied these parameters by increasing either the density or the electron temperature. These scans lead to very different results. When beta increase because of the increase in density so does the island width. However, in the case that beta is increase by increasing the electron temperature, we observe a decrease in the island width. The main mechanism for island reduction seems to be the generation of strong sheared flow associated with the magnetic island. These results seem to reflect some observations in the LHD device.

1. Introduction

Vacuum magnetic field islands in stellarators can impact plasma confinement in different ways. Large vacuum magnetic field islands can cause a serious degradation of the confinement and if they are large enough even render a device useless as a plasma confinement experiment. However, if the vacuum magnetic field islands are small, they can improve the plasma stability by causing local flattening of the pressure profile at the rational surfaces [1,2]. Magnetic islands can also improve confinement by amplification of local shear flows [3]. The presence of a small vacuum magnetic field island induces a symmetry breaking effect that allows shear flow amplification through Reynolds stress. It is even possible to consider that such sheared flow amplification can lead to the creation of a transport barrier. Therefore such magnetic islands can be used as external knobs to control stability and confinement properties of the plasma.

Since the size of the islands is critical to having a positive or negative effect on confinement, it is important to understand how the vacuum magnetic field islands are affected by the presence of the plasma and under what conditions they are amplified or reduced. In the Large Helical Device (LHD) plasma discharges, it has been observed that the size of an externally imposed island with mode number ($m = 1, n = 1$) changes with beta and collisionality in a nontrivial way [4, 5].

In this paper, we explore a possible mechanism for changing size of vacuum magnetic field island by the plasma. This mechanism consists of the coupling of the vacuum-field island with resonant resistive interchange mode instabilities. Numerical calculations using reduced magnetohydrodynamical (MHD) equations have shown that both amplification and reduction of the island size are possible.

2. Resistive pressure gradient stability model

The basic model used in studying the nonlinear interaction of the plasma with the vacuum magnetic field islands is the reduced MHD equations. This set of equations is based on the

averaging method applied to stellarator geometry [6]. Because of the different effects of the vacuum islands on temperature and density transport, we consider separate equations for the evolution of the plasma density and temperature. The detailed version of the present model has been discussed in Ref. [3]. The geometry of the system is a periodic cylinder with minor radius a and length $L_0 = 2\pi R_0$. The model is described by the following equations; the poloidal magnetic flux evolution equation:

$$\frac{1}{R_0} \frac{\partial \tilde{\psi}}{\partial t} = -\nabla_{\parallel} \tilde{\Phi} - \frac{1}{|e|n_{eq}} \left(T_{eq} \nabla_{\parallel} \tilde{n} + n_{eq} \nabla_{\parallel} \tilde{T}_e \right) + \eta \tilde{J}_z, \quad (1)$$

the perpendicular momentum balance equation:

$$\rho_m \frac{\partial \tilde{U}}{\partial t} = -\rho_m \mathbf{v}_{\perp} \cdot \nabla U - B_0 \nabla_{\parallel} \tilde{J}_z + \kappa \left(T_{eq} \frac{1}{r} \frac{\partial \tilde{n}}{\partial \theta} + n_{eq} \frac{1}{r} \frac{\partial \tilde{T}_e}{\partial \theta} \right) + \rho_m \mu \nabla_{\perp}^2 \tilde{U}, \quad (2)$$

the electron density evolution equation:

$$\frac{\partial \tilde{n}}{\partial t} = -\mathbf{v}_{\perp} \cdot \nabla n + \frac{1}{|e|} \nabla_{\parallel} \tilde{J}_z + D_{\perp} \nabla_{\perp}^2 \tilde{n}, \quad (3)$$

and the electron temperature evolution equation:

$$\frac{\partial \tilde{T}_e}{\partial t} = -\mathbf{v}_{\perp} \cdot \nabla T_e + \frac{T_{eq}}{|e|n_{eq}} \nabla_{\parallel} \tilde{J}_z + \nabla_{\parallel} (\chi_{\parallel} \nabla_{\parallel} T_e) + \chi_{\perp} \nabla_{\perp}^2 \tilde{T}_e. \quad (4)$$

Here, κ is the averaged magnetic field line curvature, \mathbf{v}_{\perp} is the perpendicular flow velocity, U is the z -component of the vorticity, ψ is the poloidal magnetic flux function, $J_z = \nabla_{\perp}^2 \psi / \mu_0 R_0$ is the parallel current, η is the resistivity, and ρ_m is the mass density. In Eqs. (1)-(4), a tilde identifies perturbed quantities, and the subindex eq identifies equilibrium quantities.

The evolution equations of the averaged electron density and temperature profiles are obtained by flux-surface averaging of Eqs. (3)-(4). The poloidal flow profile evolution equation is derived by taking the flux surface average of Eq. (2). In this equation, we assume that the dissipative term is $-\rho_m \hat{\mu} \langle U \rangle$. That is, the dissipation is caused by a drag instead of diffusion, and is due to magnetic pumping.

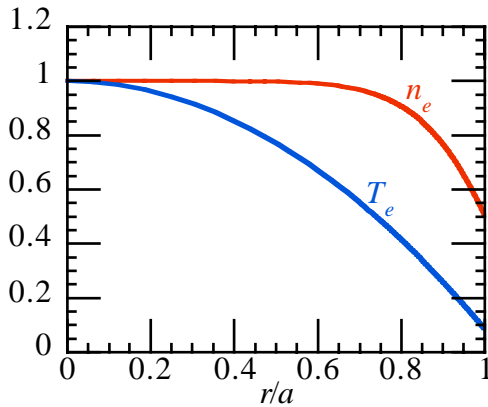


Fig. 1. Radial profiles of equilibrium density and electron temperature.

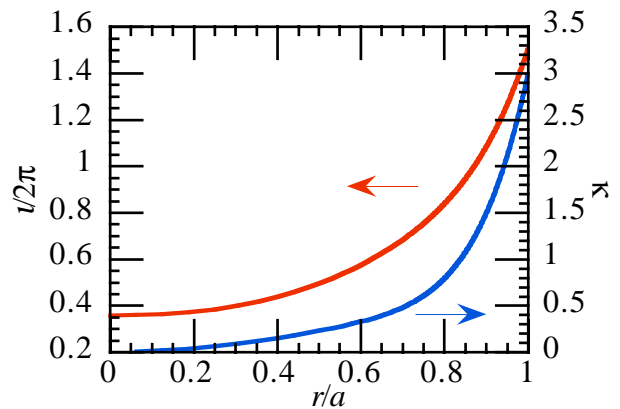


Fig. 2. Radial profiles of rotational transform and averaged magnetic field line curvature.

In the numerical calculations, we use a rotational transform, averaged magnetic field line curvature, density and temperature profiles that correspond to a shifted-in LHD configuration. These profiles are plotted in Figs. 1 and 2. The nonlinear evolution calculations are single helicity 1/1 calculations. We have included 30 poloidal components, from $m = 1$ to $m = 30$ and we have taken into account both parities. The radial grid resolution is $\Delta r/a = 10^{-3}$. The vacuum island is introduced through a non-zero boundary condition for the ($m = 1, n = 1$) component of the poloidal flux.

Because of the computing capability limitations, the values of the Lunquist number and the parallel electron conductivity are one order of magnitude smaller than the experimental values. For the reference case (case 1 in Table I), the Lunquist number, $S = \tau_R/\tau_{hp}$, is 2×10^5 , $\beta_0/2\epsilon^2 = 0.05$, the diamagnetic frequency, $\omega_{*e} = T_{eq}(0)/|e|a^2B_0$, is $4 \times 10^{-4} \tau_{hp}^{-1}$, the diffusivity coefficients are $D_{\perp} = \chi_{\perp} = \mu = 0.125 a^2/\tau_R$, and the parallel electron heat conductivity, $\chi_{\parallel} = 3.2T_e\tau_e/m_e$, is $\chi_{\parallel} = 10^6 R_0^2/\tau_R$. Here, $\tau_R \equiv a^2\mu_0/\eta(0)$ is the resistive time and $\tau_{hp} \equiv R_0\sqrt{\mu_0\rho_m/B_0}$ is the poloidal Alfvén time. The collisional flow damping rate, $\hat{\mu}$, is $2 \times 10^{-5} v_e$ for all cases considered.

Calculations have been done for different values of the peak density and temperature. These values have been increased by factors up to 4 times the standard case. In doing so, all parameters listed above have been rescaled by the corresponding factors through their dependence in temperature and density.

3. Effect of beta and collisionality on the vacuum magnetic field island

As we have shown [3], there is a poloidal rotation of the magnetic island when the imposed vacuum magnetic island is small. As the vacuum magnetic island increases for fixed value of the plasma parameters, the rotation stops and changes to an oscillatory behavior in the poloidal direction. This oscillation is around a given poloidal position and has quasiperiodic character. If we keep the vacuum magnetic island fixed and we vary the plasma parameters, for low values of the density and high temperature, there is no poloidal rotation of the island. However, as the density increases at low temperatures, the island first oscillates in a quasiperiodic way and at even higher density values there is full poloidal rotation of the island. We can expect the maximum nonlinear interaction between the vacuum island and the plasma instability in the regime where the island does not rotate. All cases considered in this paper are in this regime.

In the present numerical calculations, we have used two different values for the ($m = 1, n = 1$) component of the vacuum poloidal flux at the boundary, $\psi_b = 5 \times 10^{-4}$ and 1.28×10^{-3} ; the corresponding vacuum magnetic island widths are $W_{vac} = 0.05a$ and $0.08a$. For each value of

TABLE I

Case	Density factor	Temperature factor	$\beta_0/2\epsilon^2$	S
1	1	1	0.05	2×10^5
2	2	1	0.10	1.41×10^5
3	4	1	0.20	10^5
4	1	2	0.10	5.66×10^5
5	2	2	0.20	4×10^5

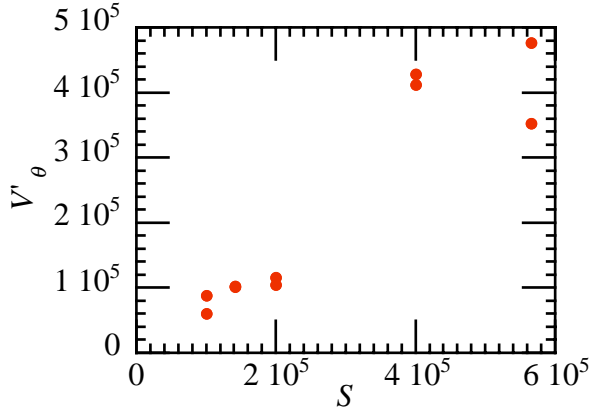


Fig. 3. Shear flow at the singular surface $q = 1$ vs. S for all cases considered in this paper.

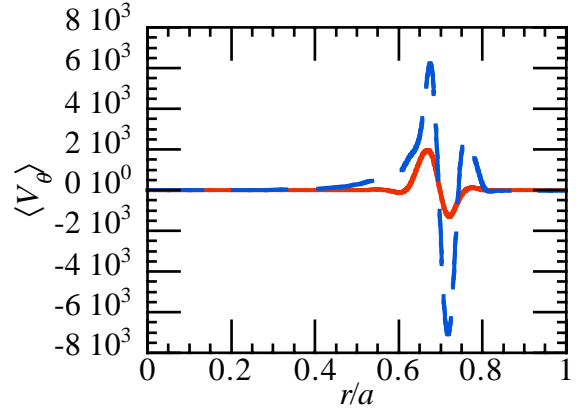


Fig. 4. Radial profile of the poloidal flow for cases 2 (solid line) and 4 (broken line) with $\psi_b = 5 \times 10^{-4}$

ψ_b , and starting from the reference case, we have increased the density and/or the electron temperature by the factors listed in Table I. In the same table we list the corresponding values of β and S .

The increase of temperature causes a decrease in collisionality and as a consequence there is an increase on the level of shear flow over the magnetic island. From this perspective, we can identify two regimes: 1) a low S regime with low sheared flow and 2) a high S regime with strong sheared flow. This correlation between S and shear flow level is shown in Fig. 3. As shown in Fig. 4 and for these two regimes, the sheared flow profile does not change much. It is essentially the level of the sheared flow that changes.

For the low sheared flow regime, when beta increases because of the increase in density so does the island width. This is shown in Fig. 5 for six different calculations corresponding to cases 1 to 3 in Table I and for the two values of the vacuum magnetic field island. However, in the high sheared flow regime, this shear flow not only causes a reduction in the level of plasma fluctuations [7], but also a reduction in the magnetic island width, even below the vacuum magnetic island size. This second regime corresponds mostly to increasing beta by increasing the electron temperature. This result is shown in Fig. 6, for the cases 4 and 5 of table I and for the two values of the vacuum magnetic field island.

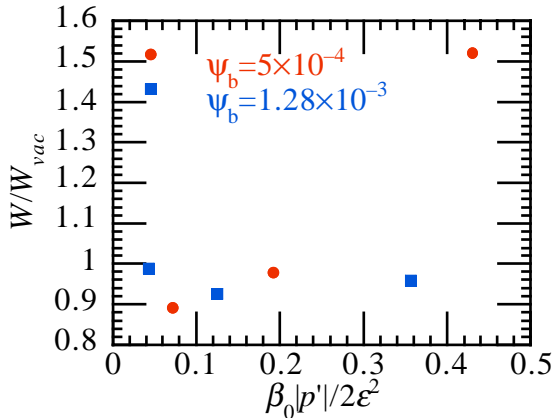


Fig. 5. Normalized width vs. local pressure gradient for cases 1 to 3.

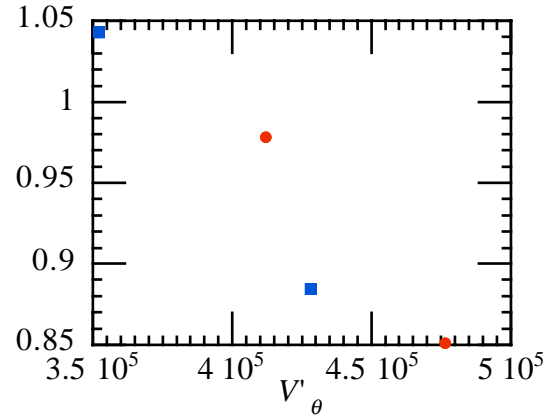


Fig. 6. Normalized width vs. local shear flow for cases 4 and 5.

The change on the island size, even if it is small due the short range of values of temperature and density variation, is real. We can see that in Fig. 7, where we have plotted the $(m = 1, n = 1)$ component of the poloidal flux function for a case of enhancement and a case of reduction of the magnetic island. There is a clear change of the value of the poloidal flux at the resonant surface.

4. Conclusions

The coupling of a vacuum magnetic field island with a resonant resistive interchange mode can cause important changes in the measured island size. For high β and high collisionality, the sheared flow damping is important and the main effect is an increase in the island size induced by β . However, at low collisionality, we have a decrease of the poloidal flow damping term. Therefore, the sheared flow associated with the magnetic island increases and this increase caused a reduction of the overall magnetic island size.

These two different ways of modifying the vacuum magnetic island by the plasma can be easily carried out in experiment by increasing β in two different ways, through increase of the density or through increase of the electron temperature. These results are consistent with the observation in the LHD experiment described in Ref. [5]. Further exploration of the high temperature, high β regime would be desirable, but this is still limited by computational capabilities.

Acknowledgments

We would like to thank Dr. Ohyabu and Dr. Ichiguchi for useful discussions and for providing us with information of LHD equilibrium profiles. This research is sponsored by the Dirección General de Investigación (Spain) under Project No. FTN2000-0924-C03. Part of this research has been carried out at Oak Ridge National Laboratory, managed by UT-Battelle, LLC, for the U.S. Department of Energy under contract number DE-AC05-00OR22725.

References

- [1] CARRERAS, B. A., et al., Phys Plasmas **8** (2001) 990.
- [2] ICHIGUCHI, K., et al., Nuclear Fusion **41** (2001) 181.
- [3] GARCIA, L., et al., Phys. Plasmas **8** (2001) 4111.
- [4] NARIHARA, K., et al., Phys. Rev. Lett. **87** (2001) 135002.
- [5] OHYABU, K., et al., Phys. Rev. Lett. **88** (2002), 055005.
- [6] GREENE, J. M., and JOHNSON, J. L., Phys. Fluids **4** (1961) 875.
- [7] BIGLARI, H., DIAMOND, P. H., and TERRY, P. W., Phys. Fluids B **2** (1990) 1.

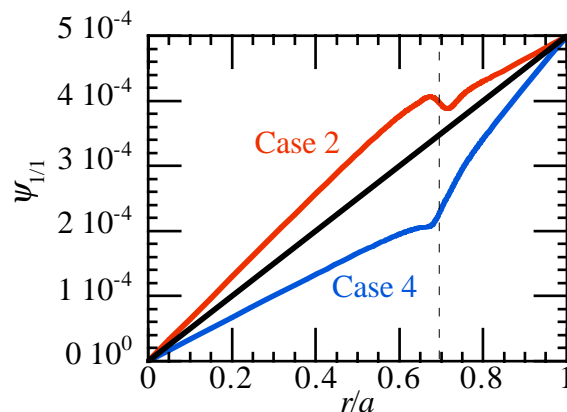


Fig. 7. Radial profile of the $(m = 1, n = 1)$ component of the poloidal flux function for cases 2 and 4 with $\psi_b = 5 \times 10^{-4}$